Chemical Science

ROYAL SOCIETY OF CHEMISTRY

EDGE ARTICLE

View Article Online
View Journal | View Issue

Cite this: *Chem. Sci.*, 2024, **15**, 2593

All publication charges for this article have been paid for by the Royal Society of Chemistry

Received 30th October 2023
Accepted 8th January 2024

DOI: 10.1039/d3sc05797f

rsc.li/chemical-science

Enantioselective nickel-catalyzed Mizoroki–Heck cyclizations of amide electrophiles†

Ana S. Bulger, ‡ Daniel J. Nasrallah, ‡ Arismel Tena Meza ‡ and Neil K. Garg *

Amide cross-couplings that rely on C–N bond activation by transition metal catalysts have emerged as valuable synthetic tools. Despite numerous discoveries in this field, no catalytic asymmetric variants have been disclosed to date. Herein, we demonstrate the first such transformation, which is the Mizoroki–Heck cyclization of amide substrates using asymmetric nickel catalysis. This proof-of-concept study provides an entryway to complex enantioenriched polycyclic scaffolds and advances the field of amide C–N bond activation chemistry.

Introduction

Metal-catalyzed cross-coupling reactions are essential tools for synthetic chemists.[1] Our laboratory and others have been interested in investigating unconventional cross-coupling partners to discover new fundamental reactivity, enable chemoselective reactions, and advance the field by expanding the synthetic toolbox.[2] One class of unconventional cross-coupling handles, acyl electrophiles[3] (Fig. 1A, **2**) are underexplored compared to traditional electrophiles, such as aryl halides and pseudohalides. Of the known acyl electrophiles, thioesters (**2a**) have been investigated the most in conventional asymmetric transition-metal catalyzed cross-couplings (*i.e.*, **2a** → **1**).[4] Anhydrides (**2b**) and acid chlorides (**2c**) have also been used in asymmetric catalysis in the context of reductive or photochemical cross-couplings (**2b–c** → **1**).[5] Recently, the far less reactive acyl electrophiles, esters[6] (**2d**) and amides[7] (**2e**), have been investigated as electrophiles in C–C and C–heteroatom bond-forming reactions. Of note, no catalytic asymmetric examples have been reported using these species as electrophiles (*i.e.*, **2d** or **2e** → **3**).

Amides (Fig. 1B, **2e**) are particularly attractive as synthetic building blocks. They are known for their pronounced stability under various reaction conditions, including hydrolysis and redox processes. Amides can also be used as directing groups in other useful processes, such as aryl C–H bond functionalization.[8] Thus, amides have the potential to be employed in synthetic sequences, then activated late-stage to access a variety of other functional groups. The pronounced stability of amides is largely attributed to resonance delocalization of the nitrogen lone pair.[9] This leads to the high kinetic barrier associated with breaking the amide C–N bond and has led to the historical avoidance of amides as versatile synthetic handles.[10] Thus, our laboratory and others[11] have been interested in expanding known reactivity of these historically underutilized functional handles under mild conditions. Our specific interests pertain to cross-coupling reactions of amides using transition-metal catalysis, which led to our first report of an amide cross-coupling, published in 2015.[7a] Subsequently, amides have become versatile electrophiles in Pd- and Ni-catalyzed cross-coupling reactions.

Mechanistically, these reactions are typically thought to proceed by oxidative addition to the amide C–N bond to generate acyl metal species **4**.[7a] Subsequent interception by a nucleophile gives rise to products **5**. Using this platform, amides can now be readily converted to functional groups such as ketones, carboxylic acids, esters, and other amides, through relatively simple net substitution processes. We questioned if the use of a chiral ligand on the metal could provide an opportunity to access enantioenriched products. Despite there being more than a hundred amide cross-couplings involving

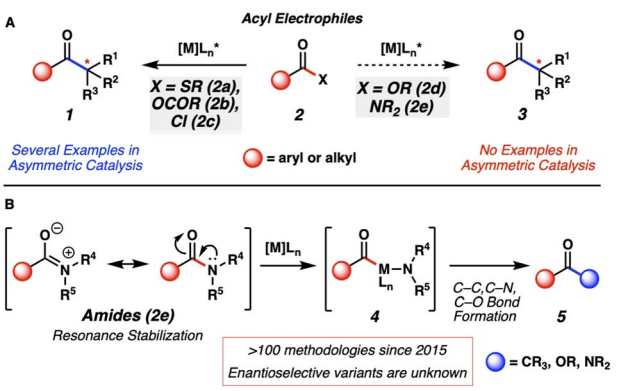

Fig. 1 (A) Asymmetric metal-catalyzed reactions of acyl electrophiles and current limitations. (B) Current state-of-the-art of amide cross-coupling reactions.

Department of Chemistry and Biochemistry, University of California at Los Angeles, Los Angeles, California 90095, USA. E-mail: neilgarg@chem.ucla.edu

† Electronic supplementary information (ESI) available. CCDC 2271421. For ESI and crystallographic data in CIF or other electronic format see DOI: https://doi.org/10.1039/d3sc05797f

‡ These authors contributed equally to this work.

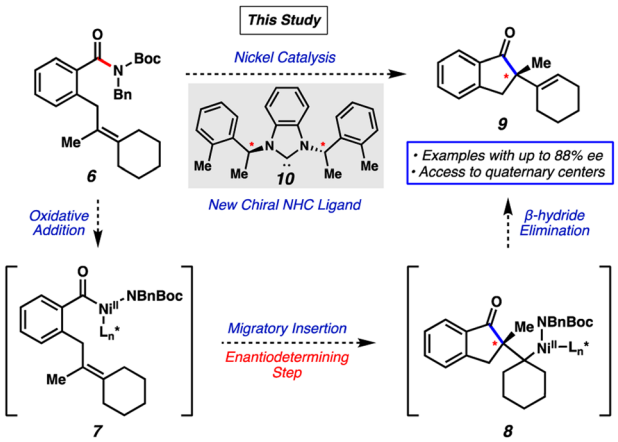

Fig. 2 Overview of the reaction design and proposed mechanism.

C–N bond activation reported since 2015,[12] asymmetric variants that utilize a chiral metal catalyst have not been discovered. Such processes would provide a new avenue in amide bond activation chemistry to allow access to enantioenriched molecules from simple amide precursors.

We envisioned that an asymmetric Mizoroki–Heck cyclization would be a suitable platform to access enantioenriched products from amide electrophiles.[13] Our reaction design, inspired by prior racemic Heck-type reactions of amide electrophiles discovered by our laboratory[7j] and Stanley's,[7l] and other asymmetric examples involving acyl-metal intermediates[14,15] is shown in Fig. 2. Representative amide substrate **6** bearing a tethered olefin would undergo oxidative addition using a metal catalyst to form acyl metal species **7**. Subsequent olefin coordination and migratory insertion (the enantiodetermining step) would furnish intermediate **8**. β-Hydride elimination would then provide the desired product **9**. Importantly, **9** would bear a stereodefined quaternary center, which is notable as quaternary stereocenters remain challenging to access and are highly sought-after motifs.[16]

Herein, we demonstrate the success of this approach, which provides the first asymmetric transition-metal-catalyzed reaction involving amide C–N bond cleavage. The transformation is enabled by the design of a new chiral N-heterocyclic carbene (NHC)[17] ligand **10** (Fig. 2) and the use of amine additives, and ultimately delivers select products containing quaternary centers in up to 88% enantiomeric excess (ee). Although currently limited in scope, this proof-of-concept study allows access to several highly complex, enantioenriched scaffolds. Moreover, this study demonstrates the ability to use catalytic amide C–N bond cleavage as an approach to achieve enantioselective synthesis.

Results and discussion

Our studies commenced by attempting the asymmetric Mizoroki–Heck cyclization using nickel catalysis (Fig. 3). Prior studies involving amide substrates with tethered olefins (*e.g.*, **11**) showed that a highly nucleophilic metal (*i.e.*, nickel[18]), accompanied by strongly electron-donating NHC ligands was required to activate the sterically encumbered and electron-rich amide C–N bond. A small library of new and known chiral NHC salts was accessible by a combination of acquisition from colleagues in academia (Fig. 3 top panel; see acknowledgements) and chemical synthesis (Fig. 3 bottom panel). Substrate **11** was utilized for initial studies and select results are shown in Fig. 3, with further results available in the ESI.†

Known chiral NHC salts **L1–L6** were tested using conditions developed for the racemic transformation[7j] to effect the desired conversion of amide **11** to indanone **12**. Despite the fact that these ligand salts have been employed in asymmetric reactions such as Ni-catalyzed annulations,[19] Pd-catalyzed C–H activation,[20] Cu-catalyzed allylic alkylations[21] and conjugate borylations,[22] they were found to be ineffective, even at elevated reaction temperatures. We attribute this lack of reactivity to the high degree of steric hindrance and structural rigidity of these

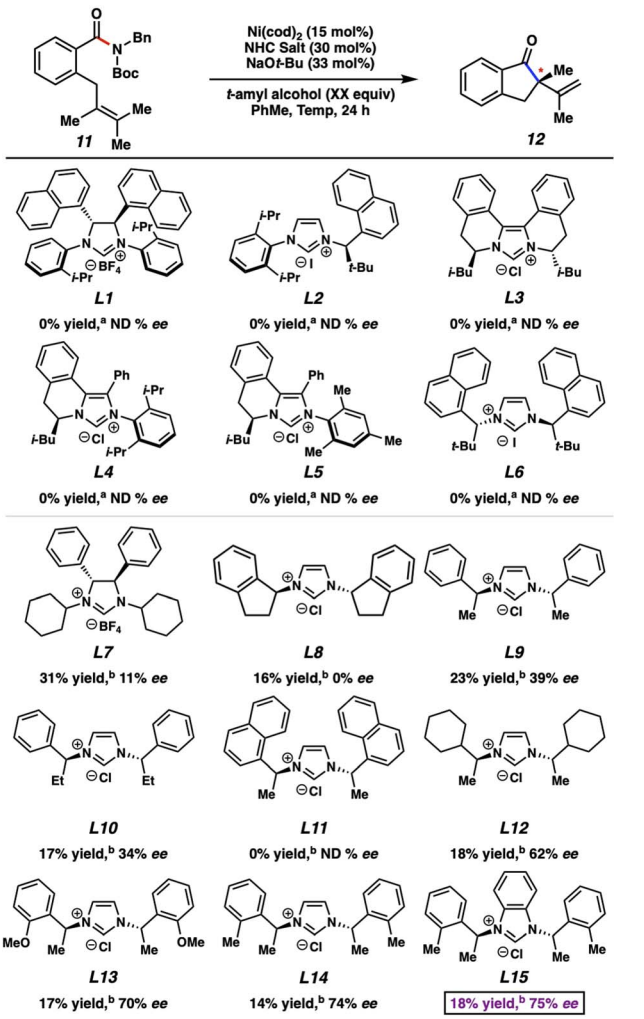

Fig. 3 Survey of chiral NHC salts with *in situ* free-basing. [a]Conditions: $Ni(cod)_2$ (15 mol%), NHC Salt (30 mol%), NaO*t*-Bu (33 mol%), PhMe (0.5 M), 100 °C; 24 h in a sealed vial. [b]Conditions: $Ni(cod)_2$ (15 mol%), NHC Salt (30 mol%), NaO*t*-Bu (33 mol%), *t*-amyl alcohol (3.0 equiv.), PhMe (0.5 M), 60 °C; 24 h in a sealed vial. [a,b]Yields determined by ^1H NMR using hexamethylbenzene as an external standard. ND is defined as not determined.

chiral NHC ligands, which could render oxidative addition challenging. In order to circumvent this issue, we examined less sterically bulky ligand salts to potentially enable oxidative addition, while still permitting selectivity in the enantiodetermining step. Using **L7–L9** we saw more promising results. Of these, **L9**, which has acyclic chiral centers in close proximity to the bound metal, gave the best combination of yield and enantioenrichment of **12** (23% yield with 39% ee). Whereas using a ligand salt with ethyl groups in place of methyl groups (*i.e.*, **L10**) led to minimal change, more pronounced effects were seen by altering the phenyl ring on **L9**. For example, the use of **L11**, which contains bulky naphthyl groups, led to no reaction, whereas the use of **L12–L14** gave product **12** with higher enantioselectivity. Finally, the use of **L15**, the benzimidazolium derivative of **L14**, led to the formation of **12** in 18% yield with 75% ee. Importantly, the two most promising NHC salts, **L14** and **L15**, were not known prior to our investigations, and NHC salts **L9**, **L12**, and **L13** had not been used previously in nickel catalysis.

To better understand the influence of different olefin substitution patterns on enantioselectivity, we tested amide substrate **6** using the most promising ligands from our aforementioned studies of substrate **11** (Fig. 4). Specifically, amide **6** bears a more sterically congested olefin with the incorporation of an additional ring. Although the use of **L7** led to poor enantioselectivity, more promising results were observed using ligand salts **L9** and **L12–L15**. The use of **L15** produced the best combination of yield and enantiomeric excess, furnishing **9** in 32% yield and 88% ee. Although beyond the scope of our present study, these ligands may prove valuable in other applications, such as in the asymmetric reactions of other electrophiles that contain strong bonds.

We attempted an initial optimization, focusing on increasing the yield of the product, using substrate **6** with **L15**. Gratifyingly, this new chiral NHC salt, **L15**, can be readily synthesized from commercially available building blocks on gram-scale and is bench-stable, rendering it an attractive choice for practical applications. Attempts to optimize the reaction by varying the stoichiometry of NaO*t*-Bu and the identity of the base did not lead to significant increase in yield (see ESI† for details). Exhaustive optimization with **L15** involving other reaction parameters, such as variation of amide *N*-substituents, solvents, and stoichiometric loading of reagents did not lead to significant catalytic turnover. Thus, in order to reduce variables in the reaction and mitigate potential unwanted base-mediated side pathways (see ESI† for details), we sought to generate the free carbene of **L15** and subsequently add it as a discrete reagent (Fig. 5). Accordingly, this would avoid the use of a base in the catalytic transformation. To our delight, carbene **10** could be generated in solution upon treatment of **L15** with KO*t*-Bu, analogous to a procedure previously reported by Cramer.[23] The identification of **10** was made using ^{13}C NMR, as **10** displays a diagnostic signal at 225.0 ppm. Carbene **10** was found to be stable under inert conditions in toluene for multiple weeks without any detectable dimerization.

Thorough variation of reaction parameters (*e.g.*, variation of *N*-substitution,[24] temperature, solvent, catalyst loading) was performed in the absence of an additive, but did not lead to improved outcomes (see ESI† for details). We turned to examining additives, with inspiration from the literature.[25] Additionally, the improvement seen in employing *t*-amyl alcohol (**13**) as an additive (Fig. 6, entry 2) compared to the lower yield observed in the absence of additive (entry 1) signified that an additive could be important in increasing the conversion of the reaction. A selection of results are shown in Fig. 6, with further results available in the ESI.† Whereas the use of other alcohols (*e.g.*, **14**) was ultimately found to give comparable results, amine additives were generally found to be most impactful, with varying results.[26] For example, when primary amines **15** and **16** were evaluated, α-tertiary amine **16** was found to improve the yield of the reaction to 42%, whereas α-primary amine **15** inhibited product formation, giving only 4% yield of **9**. Moreover, the use of amines **17–19**, which represent acyclic secondary, tertiary, and diamines, respectively, did not lead to superior yields of **9**. Cyclic amines were also evaluated. Although the use of piperidine (**20**) as an additive was not very promising (entry 9), the employment of morpholine (**21**) led to complete consumption of substrate **6** and 42% yield of indanone **9** (entry 10). The majority of the remaining mass balance was comprised of an undesired morpholine transamidation side-product. As such, the equivalents of morpholine were reduced from three to one. Using these optimized conditions

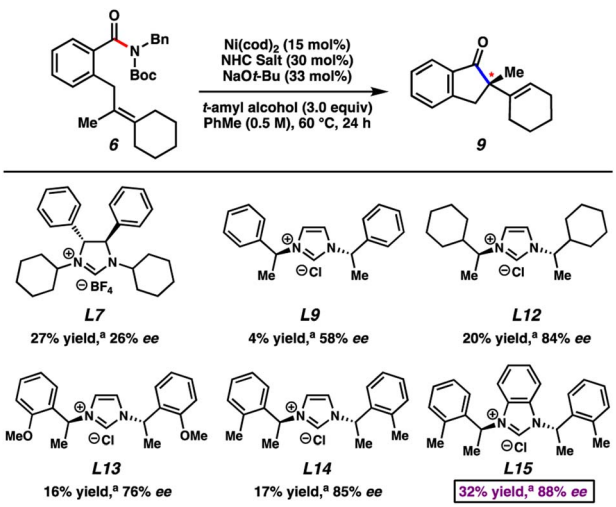

Fig. 4 Results using select chiral NHC ligand salts with amide **6**. [a]Yields determined by ^{1}H NMR using hexamethylbenzene as an external standard.

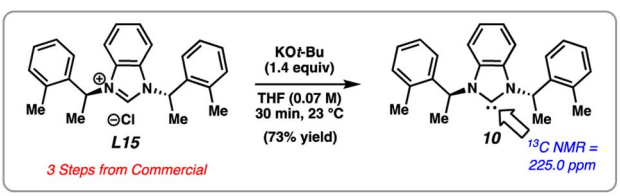

Fig. 5 Generation of free carbene **10**.

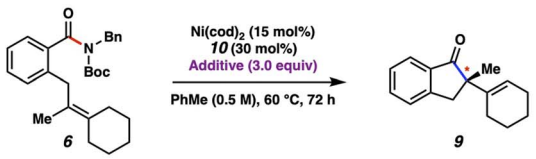

Entry	Additive	Recovered[a] 6	Yield[a] of 9	% ee
1	-	67%	11%	ND
Alcohols				
2	13 tertiary	62%	24%	ND
3	14 primary	34%	27%	ND
Primary amines				
4	15 α-primary	44%	4%	ND
5	16 α-tertiary	40%	42%	88%
Secondary amine				
6	17	30%	39%	ND
Tertiary amine				
7	18	84%	5%	ND
Diamine				
8	19	11%	34%	ND
Cyclic amines				
9	20	7%	23%	ND
10	21	0%	42%	89%
11[b]		0%	55%	88%

Fig. 6 Survey of alcohol and amine additives in the transformation. [a]Conversions and yields determined by ^{1}H NMR using hexamethylbenzene as an external standard. [b]Morpholine (1.0 equiv.).

gave indanone **9** in 55% yield with 88% ee (entry 11). It is hypothesized that the additive may have an effect on either the rate of β-hydride elimination, potentially due to reduced steric bulk around the metal, or that it could facilitate regeneration of the Ni(0) catalyst. However, future mechanistic studies would be necessary to support either conclusion as to the effect of the amine additive on the turnover-limiting step of this reaction.[27,28] Nonetheless, the findings with regard to ligand optimization and additive evaluation should provide insight into effective reaction conditions for the activation of strong-bond electrophiles in asymmetric catalytic processes.

Several substrates bearing different olefin substitution patterns were evaluated in the transformation (Fig. 7). Cyclohexylidene substrate **6** underwent the desired enantioselective transformation to deliver **9** in 54% isolated yield and 88% ee. Additionally, we demonstrated the tolerance of heterocycles through the employment of amides **22** and **24**, which gave rise to products **23** and **25**, respectively, with good enantioenrichment, albeit in modest yields. Amide **26**, bearing a sterically bulky geminal dimethyl moiety, gave rise to spirocycle **27** in good yield and moderate enantiomeric excess (80% yield with 54% ee). Additionally, an acyclic olefin (entry 5) could be tolerated in the methodology, giving rise to indanone **12** in 41% yield with 78% ee. Although the scope of the transformation is currently limited, these examples demonstrate the potential for amides to serve as acyl electrophiles in enantioselective transformations with tolerance of heterocycles and tri- or tetra-substituted olefins.

The Mizoroki–Heck cyclization provides access to complex quaternary center-containing products that are well poised to undergo further synthetic elaboration. As shown in Fig. 8, we demonstrate this virtue through the elaboration of cyclization product **9** to several scaffolds, including stereochemically complex products. One key effort involved condensation of indanone **9** with *N*-brosyl hydrazine to give brosyl hydrazone **28**. This adduct could be crystallized, which enabled the assignment of absolute stereochemistry through single crystal X-ray analysis. The absolute configuration at the quaternary stereocenter (in **28** and other derivatives of **9**) is as depicted throughout Fig. 8.

Compounds **29–31** are additional derivatives of indanone **9** that each bear a defined quaternary stereocenter (Fig. 8).

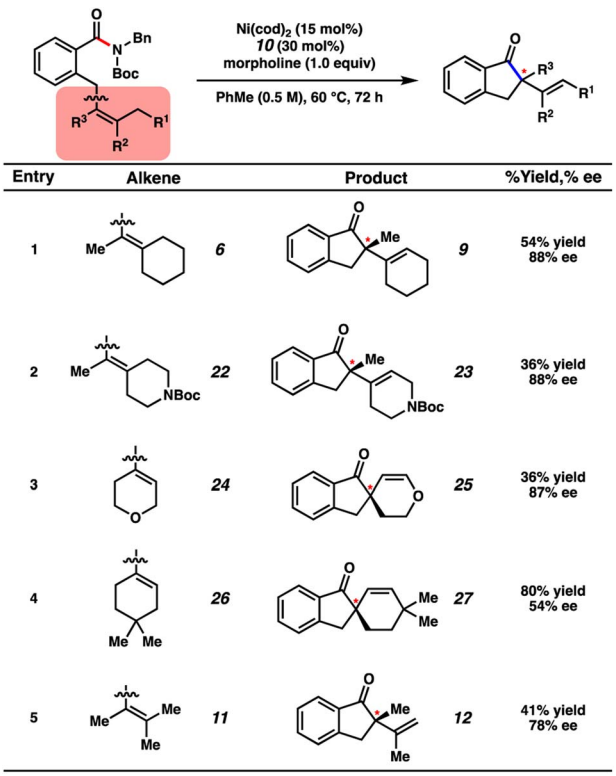

Fig. 7 Examples of methodology. Yields shown reflect the average of two isolation experiments.

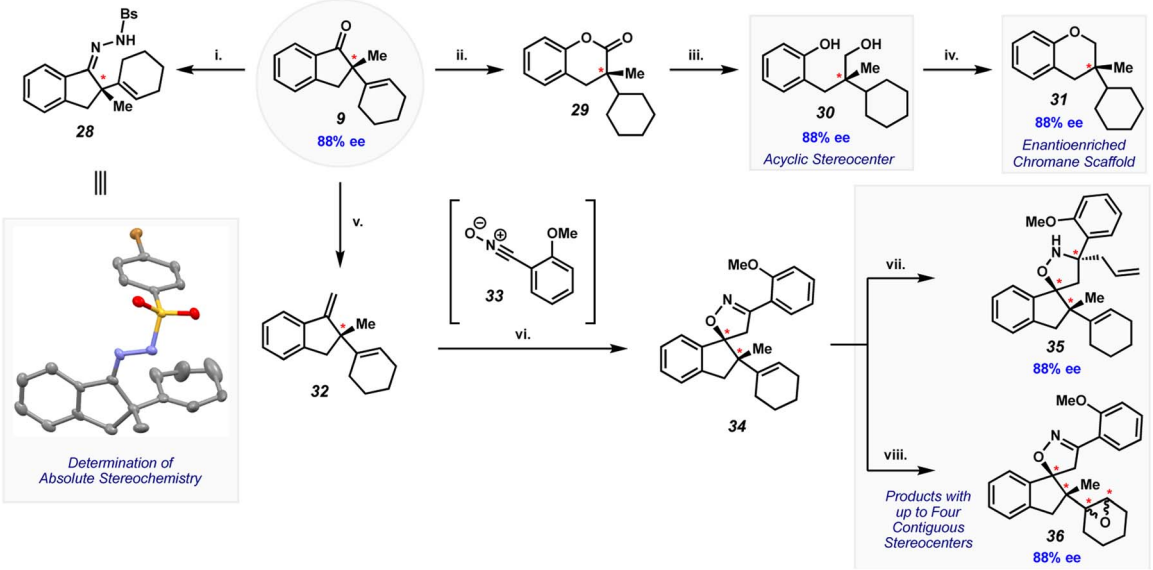

Fig. 8 Elaboration of (+)-**9** to enantioenriched compounds. (i) *N*-Brosyl hydrazine (5.0 equiv.), acetyl chloride (10 equiv.), EtOH (0.07 M), 0 → 60 °C; 72 h, 47% yield. (ii) (a) $Fe(acac)_3$ (40 mol%), PhSH (40 mol%), $PhSiH_3$ (4.0 equiv.), EtOH (0.1 M), 23 °C, 25 h. (b) TBAF (25 equiv.), 16 h, 87% yield over two steps (c) urea hydrogen peroxide (43 equiv.), TFA (19 equiv.), $BF_3{\cdot}OEt_3$ (73 equiv.), CH_2Cl_2 (0.1 M), 0 → 23 °C, 16 h, 60% yield, 1.8 : 1 rr. (iii) $LiAlH_4$ (1.5 equiv.), Et_2O (0.03 M), 0 → 23 °C, 0.5 h, quant. yield. (iv) PPh_3 (1.5 equiv.), DBAD (1.5 equiv.), CH_2Cl_2 (0.07 M), 10 °C, 3 h, quant. yield. (v) PPh_3MeBr (2.4 equiv.), *n*-BuLi (1.7 equiv.), THF (0.2 M), 23 °C, 2 h, 97% yield. (vi) 2-(Methoxy)benzohydroximinoyl chloride (2.0 equiv.), NEt_3 (2.0 equiv.), MeCN (0.1 M), 23 °C, 25 h, 79% yield, 5.3 : 1 dr. (vii) $BF_3{\cdot}OEt_2$ (3.0 equiv.), allylMgCl (15 equiv.), toluene (0.05 M), −78 °C, 2 h, 63% yield, 1.6 : 1 dr. (viii) *m*-CPBA (1.5 equiv.), $NaHCO_3$ (3.0 equiv.), CH_2Cl_2 (0.07 M), 0 °C, 2 h, 83% yield, 2.2 : 1 dr.

Although the scaffolds for these derivatives depart from that of **9**, each are readily accessible through the depicted sequence. Lactone **29** was obtained by reduction of the olefin using hydrogen-atom transfer (HAT) conditions, followed by Baeyer–Villiger oxidation. Using urea hydrogen peroxide, trifluoroacetic acid (TFA), and boron trifluoride etherate ($BF_3{\cdot}OEt_2$), the product arising from the migration of the phenyl group was observed as the major regioisomer. Subsequent reduction of lactone **29** using lithium aluminum hydride led to ring cleavage, providing diol **30** in quantitative yield. Lastly, diol **30** underwent an intramolecular Mitsunobu reaction to form chromane **31**, a common motif in bioactive molecules and pharmaceuticals.[29] The elaboration of **9** to enantioenriched products **29–31** is reminiscent of the skeletal editing paradigm,[30] which has recently received significant interest from the synthetic community.

As reflected in the remaining sequence shown in Fig. 8, we sought to elaborate indanone **9** to enantioenriched products that bear additional rings and multiple stereocenters. Wittig homologation of **9** provided olefin **32** in nearly quantitative yield. A (3 + 2) cycloaddition of **32** with *in situ*-generated nitrile oxide **33** delivered spiroheterocycle **34**. The reaction proceeds with high chemoselectivity for the more reactive styrenyl olefin in **32**. Moreover, the cycloaddition proceeds diastereoselectively (5.3 : 1 dr), with a preference for the isomer shown, presumably by approach of the 1,3-dipole from the less sterically encumbered face of the styrenyl olefin. Finally, spiroheterocycle **34** could be elaborated further to isoxazolidine **35** and epoxides **36**. The former was obtained by 1,2-addition of allyl magnesium chloride, while the latter was accessed by epoxidation of the trisubstituted cyclic olefin. In addition to retaining the quaternary stereocenter generated in the Mizoroki–Heck cyclization, products **35** and **36** contain multiple stereocenters, as well as multiple heteroatoms, rings, and functional handles for further manipulation. The results shown in Fig. 8 underscore the notion that a range of highly complex, enantioenriched scaffolds can now be accessed from amide precursors, ultimately stemming from our methodology involving amide C–N bond activation and asymmetric catalysis.

Conclusions

We have demonstrated that amides can serve as cross-coupling partners in the asymmetric transition-metal-catalyzed Mizoroki–Heck cyclization. This is notable, as more than a hundred amide cross-couplings involving C–N bond cleavage by a transition metal catalyst have been reported since 2015, but none are asymmetric. Our transformation was enabled by the development of a new NHC ligand **10**, as well as extensive reaction optimization. Through cyclization and subsequent synthetic elaborations, we show that a variety of enantioenriched polycyclic products containing difficult-to-access quaternary centers can be made, including complex compounds with up to four stereogenic centers (*i.e.*, **36**). Future studies aim to expand the scope of this reaction and develop new methods that rely on the use of amides in C–N bond cleavage reactions using asymmetric transition metal catalysis. Our studies challenge the conventional understanding of how amides can be used in chemical synthesis and, more broadly, should encourage the study of other non-traditional electrophiles in asymmetric

transformations by expanding the library of, and providing knowledge on, the types of ligands that could be employed in such transformations.

Data availability

Full details on the synthesis and characterization of compounds are accessible in the ESI.†

Author contributions

A. S. B., D. J. N., and A. T. M. designed and performed experiments and analyzed experimental data. All authors contributed to the preparation of the manuscript and participated in discussions. N. K. G. directed the investigations.

Conflicts of interest

There are no conflicts to declare.

Acknowledgements

We thank the NIH-NIGMS (R35 GM139593 for N. K. G. and Supplement for A. T. M., and F31 GM149161 for A. T. M), and the Trueblood Family (for N. K. G.), as well as the NSF (DGE-2034835 for A. S. B.), and the Foote Family (for A. S. B. and A. T. M.). We thank Dr Saeed Khan (UCLA) for X-ray analysis. These studies were supported by shared instrumentation grants from the NSF (CHE-1048804), the National Center for Research Resources (S10RR025631), and the NIH Office of Research Infrastructure Programs (S10OD028644). The authors acknowledge Professor Kendall Houk (UCLA) and Pan-Pan Chen (UCLA) for helpful discussions. The authors are also grateful to Dr Sophie Racine (UCLA) for experimental assistance and Professor Nicolai Cramer (EPFL) for gifting chiral NHC salts.

Notes and references

1 (*a*) C. Johansson Seechurn, M. O. Kitching, T. J. Colacot and V. Snieckus, *Angew. Chem., Int. Ed.*, 2012, **51**, 5062–5085; (*b*) J. Hassan, M. Sevignon, C. Gozzi, E. Schulz and M. Lemaire, *Chem. Rev.*, 2002, **102**, 1359–1470; (*c*) L. Jiang and S. L. Buchwald, in *Metal-Catalyzed Cross- Coupling Reactions*, 2nd edn, ed. A. Meijere and F. Diederich, Wiley VCH, Weinheim, 2004, pp. 699−760; (*d*) J. P. Corbet and G. Mignani, *Chem. Rev.*, 2006, **106**, 2651–2710; (*e*) E. Negishi, *Bull. Chem. Soc. Jpn.*, 2007, **80**, 233–257; (*f*) H. C. Shen, in *Application of Transition Metal Catalysis in Drug Discovery and Development: An Industrial Perspective*, ed. M. L. Crawley and B. M. Trost, Wiley, Hoboken, 2012, pp. 25−96; (*g*) L. C. Campeau and N. Hazari, *Organometallics*, 2019, **38**, 3–35; (*h*) A. Suzuki, *Angew. Chem., Int. Ed.*, 2011, **50**, 6722–6737; (*i*) E. Negishi, *Angew. Chem., Int. Ed.*, 2011, **50**, 6738–6764.

2 For select reviews on C–O, C–N and C–F bond cleaving reactions, see: (*a*) T. B. Boit, A. S. Bulger, J. E. Dander and N. K. Garg, *ACS Catal.*, 2020, **10**, 12109–12126; (*b*) S. Q. Zhang and X. Hong, *Acc. Chem. Res.*, 2021, **54**, 2158–2171; (*c*) B. A. Baviskar, P. V. Ajmire, D. S. Chumbhale, M. S. Khan, V. G. Kuchake, M. Singupuram and P. R. Laddha, *Sustainable Chem. Pharm.*, 2023, **32**, 100953; (*d*) X. Zeng and X. Huang, *Adv. Anal. Chem.*, 2022, **12**, 68–75; (*e*) M. Tian and M. Liu, *Pure Appl. Chem.*, 2021, **93**, 799–810; (*f*) J. Cornella, C. Zarate and R. Martin, *Chem. Soc. Rev.*, 2014, **43**, 8081–8097; (*g*) M. Tobisu and N. Chatani, *Acc. Chem. Res.*, 2015, **48**, 1717–1726; (*h*) F. Liu, H. J. Jiang, Y. Zhou and Z. Shi, *Chin. J. Chem.*, 2020, **38**, 855–863; (*i*) T. Zhou and M. Szostak, *Catal. Sci. Technol.*, 2020, **10**, 5702–5739; (*j*) Z. Qiu and C. J. Li, *Chem. Rev.*, 2020, **120**, 10454–10515; (*k*) T. Ahrens, J. Kohlmann, M. Ahrens and T. Braun, *Chem. Rev.*, 2015, **115**, 931–972; (*l*) L. Fu, Q. Chen and Y. Nishihara, *Chem. Rec.*, 2021, **21**, 3394–3410; (*m*) J. Becica and D. C. Leitch, *Synlett*, 2021, **32**, 641–646.

3 For select reviews on acyl electrophiles see: (*a*) J. Buchspies and M. Szostak, *Catal.*, 2019, **9**, 53; (*b*) R. Takise, K. Muto and J. Yamaguchi, *Chem. Soc. Rev.*, 2017, **46**, 5864–5888; (*c*) T. Zhou and M. Szostak, *Catal. Sci. Technol.*, 2020, **10**, 5702–5739; (*d*) L. J. Gooßen, N. Rodríguez and K. Gooßen, *Angew. Chem., Int. Ed.*, 2008, **47**, 3100–3120; (*e*) J. E. Dander and N. K. Garg, *ACS Catal.*, 2017, **7**, 1413–1423; (*f*) G. Li, S. Ma and M. Szostak, *Trends Chem.*, 2020, **2**, 914–928.

4 For this context, "conventional" is used to refer to cross-couplings employing a nucleophile and electrophile. For select studies on asymmetric transition-metal-catalyzed reactions using thioester electrophiles, see: (*a*) F. Banchini, B. Leroux, E. Le Gall, M. Presset, O. Jackowski, F. Chemla and A. Perez-Luna, *Chem.–Eur. J.*, 2023, e202301084; (*b*) R. Oost, A. Misale and N. Maulide, *Angew. Chem., Int. Ed.*, 2016, **55**, 4587–4590; (*c*) M. Liu, X. Wang, Z. Guo, H. Li, W. Huang, H. Xu and H.-X. Dai, *Org. Lett.*, 2021, **23**, 6299–6304.

5 For select studies on asymmetric transition-metal-catalyzed reductive or photochemical cross-coupling reactions using anhydride or acid chloride electrophiles, see: (*a*) A. H. Cherney, N. T. Kadunce and S. E. Reisman, *J. Am. Chem. Soc.*, 2013, **135**, 7442–7445; (*b*) H. Ji, D. Lin, L. Tai, X. Li, Y. Shi, Q. Han and L.-A. Chen, *J. Am. Chem. Soc.*, 2022, **144**, 23019–23029; (*c*) E. Gandolfo, X. Tang, S. R. Roy and P. Melchiorre, *Angew. Chem.*, 2019, **131**, 17010–17014.

6 For select recent work on transition-metal-catalyzed ester C–O bond activation and cross-couplings, see: (*a*) T. Yamamoto, J. Ishizu, T. Kohara, S. Komiya and A. Yamamoto, *J. Am. Chem. Soc.*, 1980, **102**, 3758–3764; (*b*) K. Amaike, K. Muto, J. Yamaguchi and K. Itami, *J. Am. Chem. Soc.*, 2012, **134**, 13573–13576; (*c*) L. Meng, Y. Kamada, K. Muto, J. Yamaguchi and K. Itami, *Angew. Chem., Int. Ed.*, 2013, **52**, 10048–10051; (*d*) K. Muto, J. Yamaguchi, D. G. Musaev and K. Itami, *Nat. Commun.*, 2015, **6**, 7508; (*e*) K. Muto, R. Hatakeyama, K. Itami and J. Yamaguchi, *Org. Lett.*, 2016, **18**, 5106–5109; (*f*) L. J. Gooßen and J. Paetzold, *Angew. Chem., Int. Ed.*, 2002, **41**, 1237–1241; (*g*) L. J. Gooßen and J. Paetzold, *Angew. Chem., Int. Ed.*, 2004, **43**, 1095–1098; (*h*) N. Chatani,

H. Tatamidani, Y. Ie, F. Kakiuchi and S. Murai, *J. Am. Chem. Soc.*, 2001, **123**, 4849–4850; (*i*) H. Tatamidani, K. Yokota, F. Kakiuchi and N. Chatani, *J. Org. Chem.*, 2004, **69**, 5615–5621; (*j*) H. Tatamidani, F. Kakiuchi and N. Chatani, *Org. Lett.*, 2004, **6**, 3597–3599; (*k*) N. A. LaBerge and J. A. Love, *Eur. J. Org Chem.*, 2015, **2015**, 5546–5553; (*l*) T. Ben Halima, J. K. Vandavasi, M. Shkoor and S. G. Newman, *ACS Catal.*, 2017, **7**, 2176–2180; (*m*) A. Kruckenberg, H. Wadepohl and L. H. Gade, *Organometallics*, 2013, **32**, 5153–5170; (*n*) H. Yue, L. Guo, H.-H. Liao, Y. Cai, C. Zhu and M. Rueping, *Angew. Chem., Int. Ed.*, 2017, **56**, 4282–4285; (*o*) H. Yu, L. Guo, S.-C. Lee, X. Liu and M. Rueping, *Angew. Chem., Int. Ed.*, 2017, **56**, 3972–3976; (*p*) T. Ben Halima, W. Zhang, I. Yalaoui, X. Hong, Y. Yang, K. N. Houk and S. G. Newman, *J. Am. Chem. Soc.*, 2017, **139**, 1311–1318; (*q*) L. Hie, N. Fine Nathel, X. Hong, Y.-F. Yang, K. N. Houk and N. K. Garg, *Angew. Chem., Int. Ed.*, 2016, **55**, 2810–2814; (*r*) T. Ben Halima, J. Masson-Makdissi and S. G. Newman, *Angew. Chem., Int. Ed.*, 2018, **57**, 12925–12929; (*s*) Y.-L. Zheng and S. G. Newman, *ACS Catal.*, 2019, **9**, 4426–4433; (*t*) C. W. Cheung, M. L. Ploeger and X. Hu, *Nat. Commun.*, 2017, **8**, 14878; (*u*) H. K. Banovetz, K. L. Vickerman, C. M. David, M. Alkan and L. M. Stanley, *Org. Lett.*, 2021, **23**, 3507–3521; (*v*) Y.-L. Zheng, P.-P. Xie, O. Daneshfar, K. N. Houk, X. Hong and S. G. Newman, *Angew. Chem.*, 2021, **133**, 13588–13595; (*w*) S. Yang, T. Zhou, A. Poater, L. Cavallo, S. P. Nolan and M. Szostak, *Catal. Sci. Technol.*, 2021, **11**, 3189–3197.

7 For recent articles on nickel-catalyzed reactions proceeding through amide C–N bond cleavage, see: (*a*) L. Hie, N. Fine Nathel, T. K. Shah, E. L. Baker, X. Hong, Y.-F. Yang, P. Liu, K. N. Houk and N. K. Garg, *Nature*, 2015, **524**, 79–83; (*b*) N. A. Weires, E. L. Baker and N. K. Garg, *Nat. Chem.*, 2016, **8**, 75–79; (*c*) E. L. Baker, M. M. Yamano, Y. Zhou, S. M. Anthony and N. K. Garg, *Nat. Commun.*, 2016, **7**, 11554; (*d*) B. J. Simmons, N. A. Weires, J. E. Dander and N. K. Garg, *ACS Catal.*, 2016, **6**, 3176–3179; (*e*) S. Shi and M. Szostak, *Org. Lett.*, 2016, **18**, 5872–5875; (*f*) S. Shi and M. Szostak, *Chem.–Eur. J.*, 2016, **22**, 10420–10424; (*g*) L. Hie, E. L. Baker, S. M. Anthony, J.-N. Desrosiers, C. Senanayake and N. K. Garg, *Angew. Chem., Int. Ed.*, 2016, **55**, 15129–15132; (*h*) A. Dey, S. Sasmal, K. Seth, G. K. Lahiri and D. Maiti, *ACS Catal.*, 2017, **7**, 433–437; (*i*) S. Ni, W. Zhang, H. Mei, J. Han and Y. Pan, *Org. Lett.*, 2017, **19**, 2536–2539; (*j*) J. M. Medina, J. Moreno, S. Racine, S. Du and N. K. Garg, *Angew. Chem., Int. Ed.*, 2017, **56**, 6567–6571; (*k*) X. Li and G. Zou, *Chem. Commun.*, 2015, **51**, 5089–5092; (*l*) J. A. Walker, K. L. Vickerman, J. N. Humke and L. M. Stanley, *J. Am. Chem. Soc.*, 2017, **139**, 10228–10231; (*m*) J. Hu, M. Wang, X. Pu and Z. Shi, *Nat. Commun.*, 2017, **8**, 14993; (*n*) N. A. Weires, D. D. Caspi and N. K. Garg, *ACS Catal.*, 2017, **7**, 4381–4385; (*o*) S. Shi and M. Szostak, *Synthesis*, 2017, 3602–3608; (*p*) J. E. Dander, E. L. Baker and N. K. Garg, *Chem. Sci.*, 2017, **8**, 6433–6438; (*q*) P.-Q. Huang and H. Chen, *Chem. Commun.*, 2017, **53**, 12584–12587; (*r*) T. Deguchi, H.-L. Xin, H. Morimoto and T. Ohshima, *ACS Catal.*, 2017, **7**, 3157–3161; (*s*) J. E. Dander, M. Giroud, S. Racine, E. R. Darzi, O. Alvizo, D. Entwistle and N. K. Garg, *Commun. Chem.*, 2019, **2**, 82; (*t*) M. M. Mehta, T. B. Boit, J. E. Dander and N. K. Garg, *Org. Lett.*, 2020, **22**, 1–5; (*u*) R. R. Knapp, A. S. Bulger and N. K. Garg, *Org. Lett.*, 2020, **22**, 2833–2837; (*v*) T. B. Boit, M. M. Mehta, J. Kim, E. L. Baker and N. K. Garg, *Angew. Chem., Int. Ed.*, 2021, **60**, 2472–2477; (*w*) J. Buchspies, M. Rahman and M. Szostak, *Molecules*, 2021, **26**, 188.

8 For a select example, see: G. Rouquet and N. Chatani, *Angew. Chem., Int. Ed.*, 2013, **52**, 11726–11743.

9 (*a*) *The Amide Linkage: Structural Significance in Chemistry, Biochemistry, and Materials Science*, ed. A. Greenberg, C. M. Breneman, J. F. Liebman, Wiley, Hoboken, vol. 1, 2003, pp. 33−43; (*b*) L. Pauling, R. B. Corey and H. R. Branson, *Proc. Natl. Acad. Sci. U. S. A.*, 1951, **37**, 205–211.

10 For examples of traditional amide C–N bond cleavage reactions, see: (*a*) S. Nahm and S. M. Weinreb, *Tetrahedron Lett.*, 1981, **22**, 3815–3818; (*b*) S. Balasubramaniam and I. S. Aidhen, *Synthesis*, 2008, **2008**, 3707–3738.

11 For select reviews on mild amide activation strategies, see: (*a*) G. Meng, S. Shi and M. Szostak, *Synlett*, 2016, **27**, 2530–2540; (*b*) R. Takise, K. Muto and J. Yamaguchi, *Chem. Soc. Rev.*, 2017, **46**, 5864–5888; (*c*) D. Kaiser, A. Bauer, M. Lemmerer and N. Maulide, *Chem. Soc. Rev.*, 2018, **47**, 7899–7925.

12 This number represents a conservative estimate of the array of metal-catalyzed cross-couplings developed for amide electrophiles, demonstrated by citations of our first paper that was published in 2015.

13 Initial attempts towards an intermolecular Mizoroki–Heck reaction proved unsuccessful, but will be the subject of future investigation.

14 T. Hayashi, J. Tang and K. Kato, *Org. Lett.*, 1999, **1**, 1487–1489.

15 P. Fan, Y. Lan, C. Zhang and C. Wang, *J. Am. Chem. Soc.*, 2020, **142**, 2180–2186.

16 (*a*) J. Christoffers and A. Mann, *Angew. Chem., Int. Ed.*, 2001, **40**, 4591–4597; (*b*) C. Li, S. S. Ragab, G. Liu and W. Tang, *Nat. Prod. Rep.*, 2020, **37**, 276–292.

17 N-heterocyclic carbene ligands were of particular interest for this investigation, as opposed to other ligand classes, as they are highly electron-rich and have uniquely enabled similar non-asymmetric catalytic amide activation reactions (see T. Droge and F. Glorius, *Angew. Chem., Int. Ed.* 2010, **49**, 6940–6952. for a review on NHC ligands).

18 V. P. Ananikov, *ACS Catal.*, 2015, **5**, 1964–1971.

19 (*a*) J. S. E. Ahlin and N. Cramer, *Org. Lett.*, 2016, **18**, 3242–3245; (*b*) J. S. E. Ahlin, P. A. Donets and N. Cramer, *Angew. Chem., Int. Ed.*, 2014, **53**, 13229–13233.

20 M. Nakanishi, D. Katayev, C. Besnard and E. P. Kündig, *Angew. Chem., Int. Ed.*, 2011, **50**, 7438–7441.

21 H. Seo, D. Hirsch-Weil, K. A. Abboud and S. Hong, *J. Org. Chem.*, 2008, **73**, 1983–1986.

22 D. Hirsch-Weil, K. A. Abboud and S. Hong, *Chem. Commun.*, 2010, **46**, 7525–7527.

23 J. S. E. Ahlin, P. A. Donets and N. Cramer, *Angew. Chem., Int. Ed.*, 2014, **53**, 13229–13233.

24 A variety of other *N*-substituents were employed in the transformation, including: *N*-Ph-*N*-Boc, *N*-Ph-*N*-Ts, *N*-Ph-*N*-Ms, *N*-Bn-*N*-CO_2Et, and *N*-Me-*N*-Ph, but either led to trace amounts or no observed formation of the desired product.

25 Although the exact impact of the additive on the mechanism is currently under investigation, alcohol additives have been shown to be enabling in nickel-catalyzed cross-couplings: see ref. 7*j* and M. R. Harris, L. E. Hanna, M. A. Greene, C. E. Moore and E. R. Jarvo, *J. Am. Chem. Soc.*, 2013, **135**, 3303–3306. Amine additives have also been proposed to activate low-valent nickel species toward oxidative addition in photoredox nickel catalysis: S. Gizbertz, S. Reischauer and B. Pieber, *Nat. Catal.*, 2020, **3**, 611–620.

26 The use of enantioenriched proline derivatives was also investigated; however, these attempts either resulted in low yields of the product or comparable levels of enantioselectivity.

27 Although the turnover limiting step of the reaction has not yet been elucidated, our data from ligand optimization indicate that the β-hydride elimination step or regeneration of Ni(0) could be slow. This is supported by other proposed nickel catalysis mechanisms in the literature (see ref. 18 for more explanation on the properties of nickel as a catalyst).

28 During our optimization campaign with the morpholine additive, we also found empirically that a 1 : 2 ratio of $Ni(cod)_2$: chiral ligand **10** was necessary to achieve the desired transformation. Although the reason for this ratio has not been unambiguously established, similar findings have been seen previously. In one study, it has been suggested based on computations that two NHC ligands could be implicated in the catalyst resting state (see ref. 7*a*). Alternatively, an additional NHC ligand could be enabling for reductive elimination.

29 H. C. Shen, *Tetrahedron*, 2009, **65**, 3931–3952.

30 J. Jurczyk, J. Woo, S. F. Kim, B. D. Dherange, R. Sarpong and M. D. Levin, *Nat. Synth.*, 2022, **1**, 352–364.